J Appl Physiol 99: 1822–1834, 2005.
First published July 21, 2005; doi:10.1152/japplphysiol.01183.2004.

Kinetics of O_2 uptake, leg blood flow, and muscle deoxygenation are slowed in the upper compared with lower region of the moderate-intensity exercise domain

Shelley L. MacPhee,[1,2] J. Kevin Shoemaker,[2,3] Donald H. Paterson,[1,2] and John M. Kowalchuk[1,2,3]
[1]*Canadian Centre for Activity and Aging,* [2]*School of Kinesiology, and* [3]*Department of Physiology and Pharmacology, The University of Western Ontario, London, Ontario, Canada*

Submitted 21 October 2004; accepted in final form 18 July 2005

MacPhee, Shelley L., J. Kevin Shoemaker, Donald H. Paterson, and John M. Kowalchuk. Kinetics of O_2 uptake, leg blood flow, and muscle deoxygenation are slowed in the upper compared with lower region of the moderate-intensity exercise domain. *J Appl Physiol* 99: 1822–1834, 2005. First published July 21, 2005; doi:10.1152/japplphysiol.01183.2004.—Six male subjects [23 yr (SD 4)] performed repetitions (6–8) of two-legged, moderate-intensity, knee-extension exercise during two separate protocols that included step transitions from 3 W to 90% estimated lactate threshold (θ_L) performed as a single step (S3) and in two equal steps (S1, 3 W to ~45% θ_L; S2, ~45% θ_L to ~90% θ_L). The time constants (τ) of pulmonary oxygen uptake ($\dot{V}O_2$), leg blood flow (LBF), heart rate (HR), and muscle deoxygenation (HHb) were greater ($P < 0.05$) in S2 ($\tau\dot{V}O_2$, ~52 s; τLBF, ~ 39 s; τHR, ~42 s; τHHb, ~33 s) compared with S1 ($\tau\dot{V}O_2$, ~24 s; τLBF, ~21 s; τHR, ~21 s; τHHb, ~16 s), while the delay before an increase in HHb was reduced ($P < 0.05$) in S2 (~14 s) compared with S1 (~20 s). The $\dot{V}O_2$ and HHb amplitudes were greater ($P < 0.05$) in S2 compared with S1, whereas the LBF amplitude was similar in S2 and S1. Thus the slowed $\dot{V}O_2$ response in S2 compared with S1 is consistent with a mechanism whereby $\dot{V}O_2$ kinetics is limited, in part, by a slowed adaptation of blood flow and/or O_2 transport when exercise was initiated from a baseline of moderate-intensity exercise.

oxygen uptake kinetics; femoral arterial blood flow kinetics; Doppler ultrasound; knee-extension exercise; near-infrared spectroscopy

ACCOMPANYING A RISE IN EXERCISE intensity, there is a challenge to increase the rate of oxidative phosphorylation to meet the new metabolic demand of the working muscle. To meet this demand, the respiratory and cardiovascular systems must adapt in a coordinated manner to transport O_2 from the atmosphere to the mitochondria of the exercising muscle, thus allowing oxidative phosphorylation to proceed at the required rate. Pulmonary O_2 uptake ($\dot{V}O_2$) kinetics is an index of the overall efficiency and conditioning of these integrated systems and can provide pertinent information with regard to the various mechanisms regulating O_2 delivery and O_2 utilization by skeletal muscle during exercise.

Recently, it was reported (8) that, for a given absolute increase in work rate (WR), the adaptation of $\dot{V}O_2$ during leg-cycling exercise was slower and the gain (G) (i.e., $\Delta\dot{V}O_2/\Delta$WR) was greater when exercise was initiated in the upper compared with the lower regions of the moderate-intensity exercise domain. These observations agree with those of Hughson and Morrissey (22, 23) and DiPrampero et al. (13), but differ from those of DiPrampero et al. (12) and Diamond et al. (10), who reported either a faster or similar adaptation, respectively, when comparing exercise initiated from either prior moderate-intensity exercise or rest.

Brittain et al. (8) attributed the slowing of $\dot{V}O_2$ kinetics in the upper region of the moderate-intensity domain to the bioenergetic properties of the newly recruited motor units, which were assumed to be less efficient (i.e., greater O_2 or ATP cost per contraction) with a more slowly adapting $\dot{V}O_2$ response than those motor units recruited initially at exercise onset from rest or very light exercise (i.e., lower region of the moderate-intensity domain). Hughson and Morrissey (22, 23), however, suggested that the slowed $\dot{V}O_2$ response in the upper region was related to an O_2 transport limitation. In these studies (22, 23), while slower heart rate (HR) kinetics were seen when exercise was initiated in this upper region, consistent with a slower O_2 transport, muscle blood flow adaptation was not investigated.

Near-infrared (NIR) spectroscopy (NIRS) provides continuous monitoring of the relative concentration changes in local muscle microvascular and tissue oxy- (HbO_2), deoxy- (HHb), and total (Hb_{tot}) hemoglobin (Hb)/myoglobin (Mb) during dynamic exercise. The NIRS-derived HHb signal reflects the balance between local muscle O_2 delivery and muscle O_2 utilization within the region of NIRS interrogation and, when used in combination with pulmonary $\dot{V}O_2$ and muscle blood flow measurements, provides information on the adaptation of local muscle O_2 utilization (9, 19).

Thus the purpose of the present study was to examine the adaptation of $\dot{V}O_2$ to a given change in WR initiated within different regions of the moderate-intensity exercise domain while simultaneously measuring the adaptation of leg muscle blood flow (LBF), HR, and local muscle HHb during two-legged knee-extension (KE) exercise. We hypothesized *1*) that the adaptation of both $\dot{V}O_2$ and LBF would be slowed during the transition to exercise in the upper compared with the lower region of the moderate-intensity exercise domain, and *2*) that the adaptation of muscle HHb would be similar in the upper compared with the lower region of the moderate-intensity exercise domain as a consequence of a similar adaptation of the muscle perfusion-to-O_2 consumption ratio in the two regions.

METHODS

Subjects

Six young healthy male subjects [age, 23.0 yr (SD 3.8); body mass, 75.8 kg (SD 13.0); height, 183.0 cm (SD 3.7)] volunteered to partic-

Address for reprint requests and other correspondence: J. M. Kowalchuk, Canadian Centre for Activity and Aging, School of Kinesiology, 3M Centre, The Univ. of Western Ontario, London, Ontario, Canada N6A 3K7 (e-mail: jkowalch@uwo.ca).

The costs of publication of this article were defrayed in part by the payment of page charges. The article must therefore be hereby marked "*advertisement*" in accordance with 18 U.S.C. Section 1734 solely to indicate this fact.

ipate in this study. Written consent was obtained after the subjects were informed about the experimental procedures, potential risks, and discomforts. The protocol was approved by The University of Western Ontario Health Science Review Board for Research Involving Human Subjects.

Preliminary Testing

Two-legged KE exercise was performed on a custom-built KE ergometer modified for two-legged exercise from a model described previously by Bell et al. (7). Modifications included adding a second padded bar attached to a lever arm on the Monark cycle ergometer (model 814E) to allow for alternating two-legged KE instead of single-limb KE exercise and reducing the mass of the weight pan to accommodate a lower intensity for "baseline" (BL) KE exercise.

Before the exercise tests were administered, subjects were required to come into the laboratory to become familiar with performing two-legged KE exercise. Exercise transitions were performed until the subjects were comfortable at maintaining the required cadence of 30 contractions per minute (cpm) and were able to fully relax the opposing hamstring muscles of the active limb to ensure that all work was performed solely by the knee extensors.

Subjects performed two incremental WR tests on the KE ergometer on separate days to determine peak power output, estimated lactate threshold ($\theta_{L\text{-}KE}$), and peak $\dot{V}O_2$ of the KE muscle group ($\dot{V}O_{2\ peak\text{-}KE}$). After 2 min of BL exercise at 3 W (100 g), the WR was increased to 18 W (600 g) and continued to increase by 6 W (200 g) each minute until the subject signaled that he was approaching his limit of exercise tolerance, after which the WR was increased by 3 W (100 g) each minute until the subject could no longer maintain the required cadence of 30 cpm, despite verbal encouragement from the investigator.

Data from the two incremental KE exercise tests were averaged together, and peak power output was determined as the highest WR that could be maintained at the required kicking frequency for at least 1 complete min. The $\dot{V}O_{2\ peak\text{-}KE}$ was determined as the average $\dot{V}O_2$ calculated during the final 30 s of the incremental test. The $\theta_{L\text{-}KE}$ was determined by visual inspection as the $\dot{V}O_2$ at which CO_2 production ($\dot{V}CO_2$) began to increase out of proportion in relation to $\dot{V}O_2$, along with a systematic rise in the ventilatory equivalent for $\dot{V}O_2$ (minute ventilation/$\dot{V}O_2$) and end-tidal P_{O_2} with no concomitant increase in the ventilatory equivalent for $\dot{V}CO_2$ (minute ventilation/$\dot{V}CO_2$) or decrease in end-tidal P_{CO_2}. From the results of the incremental tests, each subject was assigned a WR in the moderate-intensity domain, which would elicit a $\dot{V}O_2$ corresponding to ~90% $\theta_{L\text{-}KE}$.

Exercise Protocol

Subjects performed two separate, randomly assigned experimental protocols. Each trial began with 5 min of resting data collection with the subject sitting upright with each leg secured to the lever arms of the KE ergometer, followed by 5 min of passive exercise where the subjects' legs were moved passively while an assistant cycled on the ergometer at 30 cpm. Passive leg movement was included in this study to control for the effects of muscle mechanical factors on $\dot{V}O_2$ and muscle blood flow, as well as to minimize mechanical inertia during the transition from passive to active exercise (29). This was followed by 5-min active BL exercise. All KE exercise was performed over a 2-s duty cycle (1-s contraction, 1-s relaxation), resulting in 30 cpm for each leg in an alternating pattern.

The first protocol (S1 and S2) consisted of an active exercise transition from a BL of 3 W (100 g) to a predetermined WR corresponding to 90% $\theta_{L\text{-}KE}$ performed in two equal steps [i.e., $0.5 \cdot (90\%\ \theta_{L\text{-}KE} - 3\ W)$]. The second protocol (S3) consisted of an active exercise transition from a BL of 3 W (100 g) to a predetermined WR corresponding to 90% $\theta_{L\text{-}KE}$ performed as a single step. Subjects completed four to six repetitions of the single-step protocol and six to eight repetitions of the double-step protocol to increase the signal-to-noise ratio and thus improve the confidence of the measured responses. All exercise was performed continuously, with each step transition in WR lasting 5 min in duration.

Data Collection

Gas exchange. Gas exchange was measured breath by breath by using methods similar to those previously described (35). Briefly, inspired and expired airflow and volumes were measured by using a low-dead space (90 ml), low-resistance bidirectional turbine and volume transducer (Alpha Technologies, VMM-110). The turbine and volume transducer signal were calibrated before each test by using a syringe of known volume (3.01 liters). Respired gases were sampled continuously at the mouth (1 ml/s) and analyzed for fractional concentrations of O_2, CO_2, and N_2 by using mass spectrometry (Innovision, AMIS 2000, Lindvedvej, Demark) after calibration with precision-measured gas mixtures. Changes in gas concentrations were aligned with gas volumes by passing a bolus of gas through the system and measuring the time delay (TD) between the activation of the volume turbine and the resulting changes in fractional gas concentrations as measured by the mass spectrometer. Data were collected every 20 ms by computer, and the gas concentrations and volume data were aligned to build a profile of each breath. Breath-by-breath alveolar gas exchange was calculated by using algorithms constructed by Beaver et al. (4).

LBF. Femoral arterial mean blood velocity (MBV) was measured from the right leg by using pulsed-wave Doppler ultrasound (GE/Vingmed, System Five, 4–5 MHz, 45° angle of insonation). The ultrasound gate was positioned in the center of the artery and adjusted to ensure complete insonation of the entire vessel cross section. The ultrasound probe was positioned ~2–3 cm distal to the inguinal ligament and proximal to the femoral artery bifurcation. This location has been reported previously (26, 29) and was selected in this study to minimize turbulence from the femoral bifurcation and to avoid blood flow to the inguinal and surrounding regions.

During at least one trial for each subject, femoral arterial diameter was measured by echo-Doppler ultrasound (7.5-MHz probe) and stored on VHS videotape for later analysis. Arterial diameter was determined in triplicate at rest and during the steady state of passive and active exercise by using internal electronic calipers located within the Doppler ultrasound unit. The three-diameter measures at each time point were averaged to yield a single-diameter value for each subject at each time point. Diameter measures did not vary among any of the rest or exercise conditions, as shown previously (26, 28, 29). Because of inherent inconsistencies of presenting ECG-averaged beat-by-beat LBF or MBV (28, 42), in the present study, LBF was calculated over the 2-s duty cycle as LBF (ml/min) = MBV (cm/s)$\cdot \pi\ r^2$ (cm^2)$\cdot$60, where r is the radius of the femoral artery.

NIRS. Changes in the concentration of HbO_2, HHb, Hb_{tot} Hb/Mb and tissue oxygenation index (TOI = HbO_2/Hb_{tot}) of the vastus lateralis muscle were measured by using NIRS (Hamamatsu NIRO 300, Hamamatsu Photonics KK). The theory of NIRS is described in detail by Elwell (14), with the protocol for its use in our laboratory described by DeLorey et al. (9). Briefly, the NIR optodes were positioned 5 cm apart in an optically dense plastic holder and secured to right vastus lateralis muscle equidistant from the lateral epicondyle and the greater trochanter of the femur. Optodes were held in place with tape and covered with an optically dense black sleeve to minimize the intrusion of extraneous light and loss of NIR light from the field of interrogation. The thigh, with attached optodes and covering, was wrapped with an elastic bandage to prevent movement of the optodes while still allowing for leg movement and blood velocity data collection. The intensity of incident and transmitted light was recorded continuously at 2 Hz and, along with the relevant specific extinction coefficients and estimated optical path length, used for online estimation and display of changes in concentration from the zero-set during resting BL of HbO_2, HHb, Hb_{tot}, and TOI of the vastus

lateralis muscle. The raw attenuation signals were transferred to a computer and stored for later analysis.

HR and mean arterial pressure. HR was recorded continuously by using a three-lead ECG. Mean arterial pressure (MAP) was measured with a pneumatic finger cuff (Ohmeda 2300 Finapres BP Monitor) worn on the left hand and placed at the level of the femoral artery to estimate perfusion pressure. Femoral artery vascular conductance (VC) was calculated as $LBF \cdot MAP^{-1}$. HR and MAP data were transferred and stored on computer for later analysis.

Data Analysis

$\dot{V}O_2$, LBF, HR, and VC data were filtered for erroneous data points (using the criterion of data points lying outside four standard deviations of the local mean) and linearly interpolated on a second-by-second basis. Data from each repetition of a similar protocol were time aligned to the onset of exercise and ensemble averaged to yield a single response for each subject for a given protocol. Data subsequently were averaged every 10 s to further visualize the true, underlying physiological response profile to the step increase in WR.

The resulting data were modeled by using a nonlinear, least squares regression fitting procedure (Microcal, Origin) with a monoexponential function of the form:

$$Y_{(t)} = Y_{(BL)} + Amp\{1 - e^{-[(t-TD)/\tau]}\}$$

where Y represents $\dot{V}O_2$, LBF, HR, or VC at any time (t); BL is the steady-state BL value of Y determined before each step increase in WR; Amp is the amplitude of the increase in Y above the BL value; τ is the time constant defined as the time taken for Y to increase to a value equivalent to 63% of Amp; and TD is the time delay.

For $\dot{V}O_2$, the fitting window began after the "cardiodynamic" (phase I) phase and ended at the start of the transition to another WR [i.e., phase (I-II) $\leq t = 300$ s]. The functional G of the responses was calculated as $\Delta\dot{V}O_2/\Delta WR$ and reflects the O_2 cost of the activity (i.e., $ml \cdot min^{-1} \cdot W^{-1}$). For LBF, HR, and VC, data were modeled from the first data point after the step transition in WR and fit to the end of the 5-min exercise transition.

The NIRS-derived HbO_2, HHb, Hb_{tot}, and TOI data were time aligned, ensemble averaged, and averaged to 10-s time bins to elicit a single response for each subject. Also, the time-averaged NIRS signals were "normalized" such that the BL value for S1 and S3 was adjusted to "zero," and thus the NIRS-derived data are presented as a change [Δoptical density (OD) units] from the BL value. In addition, a "true" TD (HHb-TD) before an increase in HHb after exercise onset was determined by using second-by-second data and was defined as the time required for the HHb signal to increase by 1 SD above the mean of the pretransition BL; the HHb-TD was calculated as the average of the individual repetitions for each subject. The HHb data then were fit from the time of initial increase in HHb above BL (i.e., after the HHb-TD) to the end of the exercise transition using the same monoexponential model and fitting criteria, as described above. As shown previously (9), fitting of the NIRS-derived HHb signal with a monoexponential function provides a reasonable estimate of the time course of muscle deoxygenation (i.e., effective τ). Also, the time course for the overall change in HHb was determined as the sum of the HHb-TD and the effective HHb-τ [mean response time (MRT)].

The goodness of fit of the model to the data was estimated by using both the χ^2 test and inspection of the randomness of the residuals, with special attention placed on the initial transient response. The 95% confidence interval (C_{95}) of the estimated τ for each variable was established for each step transition after first establishing the best-fit model parameters for the response and then fixing the parameter estimates for BL, Amp, and TD.

Statistical Analysis

The kinetic parameter estimates for each variable were analyzed by using a one-way ANOVA for repeated measures. A significant F ratio was further analyzed by using Tukey's post hoc analysis. Statistical significance was accepted at $P < 0.05$. All values are reported as means (SD).

RESULTS

The physical characteristics of each subject and summary from the two incremental exercise tests are presented in Table 1. The estimated θ_L occurred at ~65% (SD 2) $\dot{V}O_{2\ peak\text{-}KE}$. The BL WR was 3 W, and the ΔWR for each of S1 and S2 [15.5 W (SD 1.2)] was 50% of the ΔWR for S3 [31.0 W (SD 2.4)], as required by the protocol.

$\dot{V}O_2$ Kinetics

The adaptation of $\dot{V}O_2$ during the double- (S1, S2) and single-step (S3) protocols for a representative subject is presented in Fig. 1, *A* and *B*. For all subjects, resting $\dot{V}O_2$ was 0.41 l/min (SD 0.03) and increased ($P < 0.05$) to 0.48 l/min (SD 0.04) during passive exercise and to 0.63 l/min (SD 0.01) during active KE exercise at the 3-W BL (Table 2).

Parameter estimates of the $\dot{V}O_2$ kinetic response are presented in Table 2. The τ of the fundamental phase II $\dot{V}O_2$ response ($\tau\dot{V}O_2$) was greater ($P < 0.05$) in S2 [52 s (SD 10)] than S1 [24 s (SD 3)] and S3 [28 s (SD 2)], with this trend seen in all six subjects (Fig. 2*A*). The "between-region" effect size for $\tau\dot{V}O_2$ was greater than the C_{95} for all $\tau\dot{V}O_2$ parameter estimates (Table 2).

For a given increase in WR, the $\dot{V}O_2$ Amp was greater ($P < 0.05$) in S2 [0.28 l/min (SD 0.03)] than S1 [0.21 l/min (SD 0.02)]; the combined S1+S2 $\dot{V}O_2$ Amp and the end-exercise $\dot{V}O_2$ were not different from values seen in S3 (Table 2). The functional G ($\Delta\dot{V}O_2/\Delta WR$) for S2 [18.1 $ml \cdot min^{-1} \cdot W^{-1}$ (SD 2.7)] was greater ($P < 0.05$) than that for S1 [13.5

Table 1. *Subject characteristics*

Subject No.	Age, yr	Height, cm	Body mass, kg	$\dot{V}O_{2peak\text{-}KE}$, l/min	$\theta_{L\text{-}KE}$, l/min	S1 $\dot{V}O_2$, $\%\theta_{L\text{-}KE}$	S2 $\dot{V}O_2$, $\%\theta_{L\text{-}KE}$	S3 $\dot{V}O_2$, $\%\theta_{L\text{-}KE}$
1	22	185.0	84.0	1.79	1.20	69.8	94.9	92.8
2	22	180.0	64.0	1.93	1.31	64.8	89.2	83.2
3	31	178.0	84.0	2.24	1.40	63.6	82.0	79.2
4	22	188.0	93.2	1.97	1.36	71.9	91.0	88.4
5	22	185.0	62.5	2.02	1.28	60.8	84.1	82.5
6	21	181.5	66.8	2.37	1.43	50.5	66.7	67.5
Mean	23.0	183.0	75.8	2.05	1.33	63.6	84.6	82.3
SD	3.8	3.7	13.0	0.21	0.08	7.6	1.0	8.7

$\dot{V}O_2$, pulmonary O_2 uptake; $\dot{V}O_{2peak\text{-}KE}$, peak $\dot{V}O_2$ for two-legged knee-extension exercise; $\theta_{L\text{-}KE}$, estimated lactate threshold for two-legged knee-extension exercise; S1 and S2, double-step protocol; S3, single-step protocol.

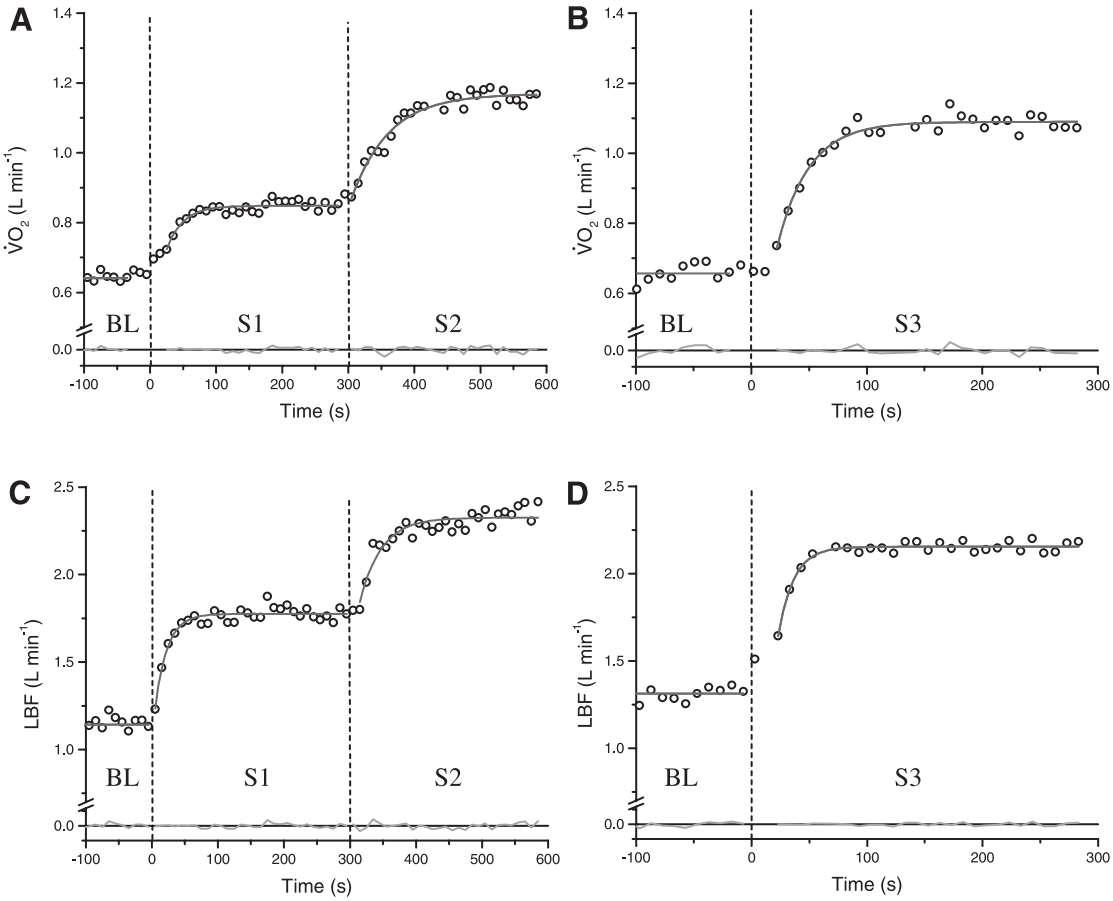

Fig. 1. Adaptation of pulmonary O_2 uptake ($\dot{V}O_2$; *A* and *B*) and leg blood flow (LBF; *C* and *D*) during a double-step (S1, S2) and single-step (S3) protocol in a representative subject. Also shown are the line of best fit and residuals of the monoexponential fit. The response profile represents an average of 6 trials, with each datum presented as a 10-s average of 1-s interpolated data. Dashed lines indicate a transition in exercise intensity. BL, baseline.

Table 2. *Parameter estimates of the on-transient $\dot{V}O_2$, LBF, and HR response to the three moderate-intensity step protocols*

Protocol	Rest, l/min	Passive, l/min	BL, l/min	Amp, l/min	TD, s	τ, s	C_{95}, s	EE, l/min	Gain, ml·min^{-1}·W^{-1}	(ΔLBF·2)/Δ $\dot{V}O_2$, liter blood/liter O_2
					$\dot{V}O_2$					
S1	0.42 (0.03)	0.48 (0.06)	0.63 (0.07)*†	0.21 (0.02)*†	10 (7)	24 (3)*	5 (1)†	0.84 (0.09)*†	13.51 (1.03)*	
S2			0.84 (0.09)*‡	0.28 (0.03)*‡	3 (3)‡	52 (10)*‡	6 (1)‡	1.12 (0.12)*	18.10 (2.71)*‡	
S3	0.40 (0.03)	0.47 (0.05)	0.63 (0.06)‡	0.46 (0.03)†‡	13 (4)‡	28 (2)‡	3 (0)†‡	1.09 (0.08)†	14.90 (1.11)‡	
					LBF					
S1	0.26 (0.04)	0.40 (0.06)	1.03 (0.08)*	0.59 (0.04)†	3 (4)	21 (2)*	4 (2)	1.62 (0.10)*†		5.7 (0.20)*†
S2			1.62 (0.10)*‡	0.63 (0.09)‡	4 (8)	39 (5)*‡	4 (3)	2.26 (0.12)*‡		4.56 (0.45)*
S3	0.25 (0.04)	0.39 (0.10)	1.06 (0.15)‡	1.06 (0.12)†‡	5 (6)	20 (5)‡	4 (2)	2.13 (0.09)†‡		4.64 (0.31)†

	Rest, beats/min	Passive, beats/min	BL, beats/min	Amp, beats/min	TD, s	τ, s	C_{95}, s	EE, beats/min
				HR				
S1	72 (5)	71 (5)	77 (4)*	9 (2)*†	3 (6)	21 (8)*	4 (1)	86 (5)*†
S2			86 (5)*‡	12 (3)*‡	−4 (4)	42 (10)*‡	6 (2)	98 (7)*‡
S3	70 (8)	68 (8)	75 (7)‡	18 (3)†‡	−2 (2)	16 (7)‡	6 (4)	93 (8)†‡

Values are means (SD). Rest, passive (passive exercise), and BL (baseline exercise at 3 W) values are in l/min for $\dot{V}O_2$ and leg blood flow (LBF) and in beats/min for heart rate (HR); Amp, amplitude, or increase in $\dot{V}O_2$ (l/min), LBF (l/min), or HR (beats/min) during step increase in work rate (WR); TD, time delay; τ, time constant; C_{95}, 95% confidence interval; EE, end-exercise $\dot{V}O_2$ (l/min), LBF (l/min), or HR (beats/min); gain, change in (Δ) $\dot{V}O_2$/ΔWR. Significant difference between *S1 and S2, †S1 and S3, and ‡S2 and S3 ($P < 0.05$ ANOVA for repeated measures and Tukey post hoc analysis).

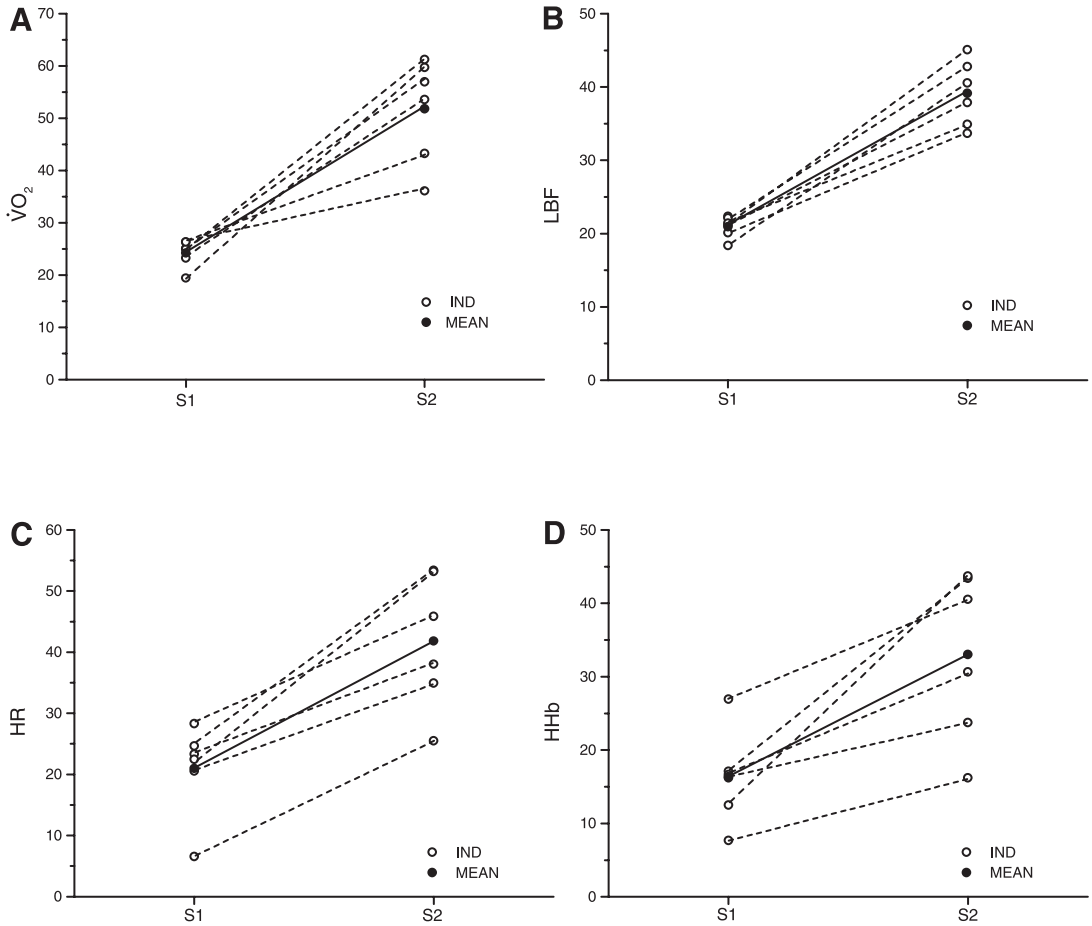

Fig. 2. Individual (IND; open symbols) and group mean (solid symbols) time constants (τ) for pulmonary $\dot{V}O_2$ ($\tau\dot{V}O_2$; *A*), LBF (τLBF; *B*), heart rate (τHR; *C*), and near-infrared spectroscopy (NIRS)-derived muscle deoxygenation (τHHb; *D*) for step transitions initiated in the lower (S1) and upper (S2) regions of the moderate-intensity exercise domain.

$ml \cdot min^{-1} \cdot W^{-1}$ (SD 1.0)] or S3 [14.9 $ml \cdot min^{-1} \cdot W^{-1}$ (SD 1.1)].

LBF Kinetics

The adaptation of LBF during the double- (S1, S2) and single-step (S3) protocols for a representative subject is presented in Fig. 1, *C* and *D*. Femoral arterial diameter [9.86 mm (SD 0.60)] did not change over the course of the rest-exercise transitions, and thus increases in blood flow changes were related only to increases in blood velocity. For all subjects, resting LBF averaged 0.26 l/min (SD 0.04) and increased ($P < 0.05$) to 0.40 (SD 0.04) and 1.05 l/min (SD 0.12) during passive exercise and active KE exercise at 3 W, respectively (Table 2).

Parameter estimates of the LBF response are presented in Table 2. At the onset of each exercise transition, femoral arterial blood flow increased exponentially toward a new steady state. The τLBF in S2 [39 s (SD 5)] was greater ($P < 0.05$) than τLBF in S1 [21 s (SD 2)] or S3 [20 s (SD 5)], a trend seen in all six subjects (Fig. 2*B*). The "between-region" differences in τLBF were greater than the C_{95} for all τLBF parameter estimates.

The LBF Amp for S1 [0.59 l/min (SD 0.04)] and S2 [0.61 l/min (SD 0.09)] were not different; the combined S1+S2 LBF Amp [1.22 l/min (SD 0.10)] was greater ($P < 0.05$) than that for S3 LBF Amp (Table 2). End-exercise LBFs for each of the transitions were different ($P < 0.05$) (Table 2). The increase in LBF for a given increase in $\dot{V}O_2$ ($\Delta LBF \cdot 2/\Delta\dot{V}O_2$) was lower ($P < 0.05$) in S2 [4.56 $l \cdot min \cdot l^{-1} \cdot min^{-1}$ (SD 0.45)] and S3 [4.64 $l \cdot min \cdot l^{-1} \cdot min^{-1}$ (SD 0.31)] than in S1 [5.70 $l \cdot min \cdot l^{-1} \cdot min^{-1}$ (SD 0.20)].

The $\dot{V}O_2$-(LBF·2) relationship was highly correlated ($P < 0.05$; $r^2 = 0.85$; Fig. 3); the slope and intercept of the relationship were 5.76 $l \cdot min \cdot l^{-1} \cdot min^{-1}$ and −1.99 l/min, respectively.

HR Kinetics

The adaptation of HR during the double- (S1, S2) and single-step (S3) protocols for a representative subject is shown in Fig. 4, *A* and *B*. HR was not different at rest [71 beats/min (SD 6)] and passive exercise [70 beats/min (SD 6)] but increased ($P < 0.05$) during the active BL exercise at 3 W [76 beats/min (SD 6)].

Parameter estimates for HR kinetics are presented in Table 2. The τHR was greater ($P < 0.05$) in S2 [42 s (SD 10)] than in S1 [21 s (SD 8)] and S3 [16 s (SD 7)], a response seen in all six subjects (Fig. 2*C*). Differences in τHR between regions were greater than the C_{95} for all τHR parameter estimates. The HR Amp and end-exercise HR for each transition all were

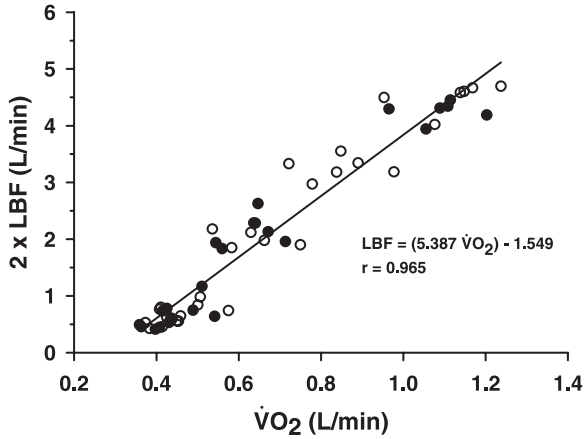

Fig. 3. Relationship between $\dot{V}O_2$ and LBF ($\times$ 2) during the double- (○) and single-step (●) transitions within the moderate-intensity exercise domain. The regression line for the relationship is also included.

different ($P < 0.05$) (Table 2); the combined S1+S2 HR Amp [20 (SD 5)] was not different from the S3 HR Amp.

MAP and Leg VC

The adaptation of MAP during the double- (S1, S2) and single-step (S3) protocols for a representative subject is presented in Fig. 4, *C* and *D*. MAP at rest [114 mmHg (SD 16)] and during passive exercise [114 mmHg (SD 6)] were similar but lower ($P < 0.05$) than during active KE exercise at the 3 W [119 mmHg (SD 5)] (Table 3). MAP Amp and end-exercise MAP were not different among the exercise transitions (Table 3).

The adaptation of leg VC during the double- (S1, S2) and single-step (S3) protocols for a representative subject is presented in Fig. 4, *E* and *F*. VC increased ($P < 0.05$) from rest [2.3 ml·min^{-1}·mmHg^{-1} (SD 0.4)] to passive exercise [3.8 ml·min^{-1}·mmHg^{-1} (SD 0.9)] to active KE exercise at 3 W [8.8 ml·min^{-1}·mmHg^{-1} (SD 1.0); Table 4].

Parameter estimates of the VC kinetic response are presented in Table 4. The τVC for S2 [34 s (SD 15)] was greater ($P < 0.05$) than for S1 [16 s (SD 3)] and S3 [17 s (SD 4)]. The VC Amp for S1 and S2 were not different and were less ($P < 0.05$) than the VC AMP for S3; the combined S1+S2 VC Amp [8.5 ml·min^{-1}·mmHg^{-1} (SD 1.3)] was similar to S3 VC Amp (Table 4). End-exercise VC for S2 and S3 were not different, and both were greater ($P < 0.05$) than the end-exercise VC for S1 (Table 4).

NIRS Response

The adaptation of the concentration changes for NIRS-derived HHb, HbO_2, and Hb_{tot} during the on-transient of a double- (S1, S2) and a single-step (S3) protocols for a representative subject is presented in Fig. 5. The pretransition BL HHb values for S1 and S3 were not different, and both were lower ($P < 0.05$) than S2.

Parameter estimates for the HHb kinetic response are presented in Table 5. The TD before an increase in HHb signal above pretransition BL (TD-HHb) was less ($P < 0.05$) for S2 [14 s (SD 7)] than for S1 [20 s (SD 4)] and S3 [17 s (SD 3)]. After the TD-HHb, the HHb increased exponentially toward a new steady state; the τHHb for S2 [33 s (SD 11)] was greater ($P < 0.05$) than the τHHb for S1 [16 s (SD 6)] and S3 [14 s (SD 5)], a response seen in all six subjects (Fig. 2*D*). The differences in τHHb between transitions were greater than C_{95} for the τHHb parameter estimates (Table 5). Also, the MRT for the HHb response (MRT = TD-HHb + τHHb) was greater ($P < 0.05$) in S2 [47 s (SD 10)] than in S1 [36 s (SD 7)] or S3 [31 s (SD 4)].

The HHb Amp and end-exercise HHb in S2 and S3 were not different, and both were greater ($P < 0.05$) than respective values seen in S1; the combined S1+S2 HHb Amp [7.9 (SD 2.2) OD units] was not different from the S3 HHb Amp. The ΔHHb/$\Delta\dot{V}O_2$ was greater in S2 than in S1 or S3 (Table 5).

The normalized HbO_2 at BL was not different among the three conditions [S1, 0.08 OD units (SD 0.14); S2, −1.06 OD units (SD 1.64); S3, 0.07 OD units (SD 0.21)]. The HbO_2 decreased transiently below BL values at the onset of each step increase in WR but returned to BL values by end-exercise.

The normalized Hb_{tot} at BL was greater ($P < 0.05$) for S2 [2.52 OD units (SD 1.60)] than for S1 [−0.01 OD units (SD 0.14)] or S3 [−0.05 OD units (SD 0.13)]. The Hb_{tot} Amp was greater ($P < 0.05$) in S2 [4.92 OD units (SD 1.18)] and S3 [5.99 OD units (SD 2.92)] than in S1 [2.52 OD units (SD 1.72)].

Relationship between the Adaptations of $\dot{V}O_2$, LBF, HR, and HHb

The relationships between the adaptations of $\dot{V}O_2$, LBF, HR, and HHb are shown in Fig. 6. During S1, the $\tau\dot{V}O_2$ [24 s (SD 3)], τLBF [21 s (SD 2)], and τHR [21 s (SD 8)] were not different from each other, but were less ($P < 0.05$) than the MRT-HHb [36 s (SD 7)]. During S2, $\tau\dot{V}O_2$ [52 s (SD 10)] was greater ($P < 0.05$) than τLBF [39 s (SD 5)] but was not different from τHR [42 s (SD 11)] and MRT-HHb [47 s (SD 10)]; no differences were seen between τLBF, τHR, and MRT-HHb. During S3, $\tau\dot{V}O_2$ [28 s (SD 2)] and MRT-HHb [31 s (SD 4)] were greater ($P < 0.05$) than τLBF [20 s (SD 5)] and τHR [16 s (SD 7)]; the τLBF and τHR were similar.

DISCUSSION

This study examined the adaptation of $\dot{V}O_2$ in humans to a given change in WR within different regions of the moderate-intensity exercise domain, while simultaneously measuring the adaptation of LBF, HR, and muscle deoxygenation during two-legged KE exercise. As a consequence of the integrative approach used in this study, we were able to determine the relationships between the metabolic adaptations ($\dot{V}O_2$, HHb) to exercise initiated in different regions of the moderate-intensity domain along with central (HR) and peripheral (LBF, VC) cardiovascular adaptations and regional muscle microvascular (HbO_2, Hb_{tot}) adaptations. The major new findings of this study were that, during KE exercise, for a given change in WR initiated in the upper (S2) compared with the lower regions (S1) of the moderate-intensity domain: *1*) the kinetics of pulmonary $\dot{V}O_2$ ($\tau\dot{V}O_2$) were slowed and the functional *G* ($\Delta\dot{V}O_2/\Delta$WR) of the response was greater; *2*) the kinetics of HR (τHR), femoral arterial blood flow (τLBF), and leg vascular conductance (τVC) were slowed; and *3*) the kinetics of muscle deoxygenation (τHHb; MRT-HHb) were slowed, the TD before an increase in muscle deoxygenation was reduced, the Amp of muscle deoxygenation (HHb Amp) and the in-

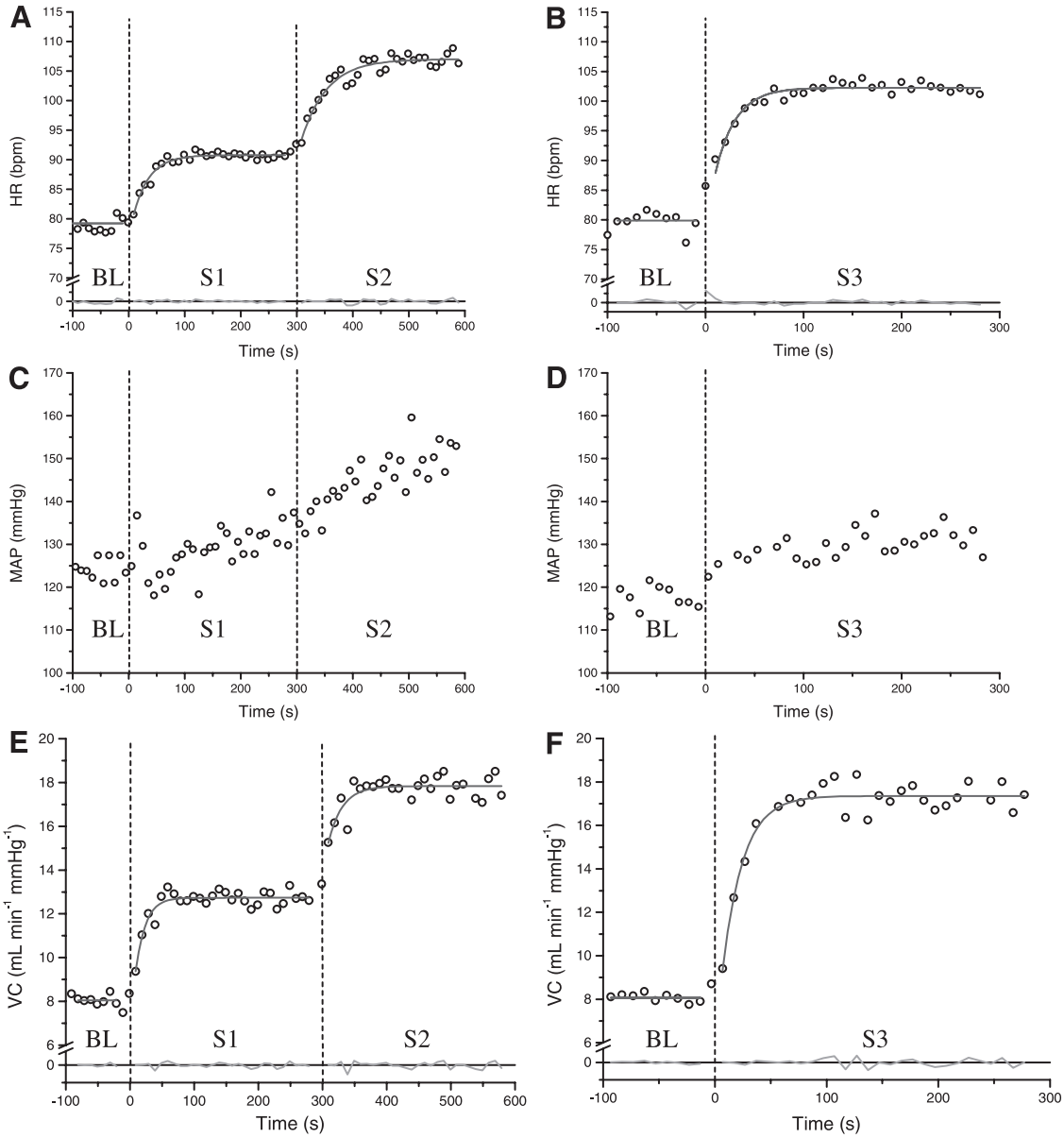

Fig. 4. Adaptation of HR (*A* and *B*), mean arterial pressure (MAP; *C* and *D*), and leg vascular conductance (VC; *E* and *F*) to double- (S1, S2) and single-step (S3) protocols. Also shown are the line of best fit and residuals of the monoexponential fit. The response profile represents an average of 6 trials, with each datum presented as a 10-s average of 1-s interpolated data. Dashed lines indicate a transition in exercise intensity. bpm, Beats/min.

crease in HHb relative to the increase in $\dot{V}O_2$ ($\Delta HHb/\Delta\dot{V}O_2$) were greater.

Our laboratory has previously shown (8) that, during two-legged cycling exercise, the adaptation of $\dot{V}O_2$ is slower in the upper compared with the lower regions of the moderate-intensity domain. In the present study, a two-legged KE exercise model was used to allow us to restrict exercise to the quadriceps muscle group (30) and to stabilize the upper leg to enable measurements of femoral arterial blood flow to the active quadriceps muscle during dynamic exercise. Also, with the two-legged KE model, a relatively larger muscle mass and greater exercise intensity could be used while still remaining in the moderate-intensity domain (compared with single-leg KE or arm cycling), thereby allowing for a greater Amp in the $\dot{V}O_2$ and LBF response and thus more confidence in the kinetic analyses and parameter estimations during the exercise transients.

In the present study, constant-load KE exercise at ~33 W (for S2 and S3) resulted in end-exercise steady-state values of

Table 3. *Parameter estimates of MAP during three moderate-intensity knee-extension exercise transitions*

Protocol	Rest	Passive	BL	Amp	EE MAP
S1	110 (10)	113 (8)	118 (4)*	7 (2)	125 (5)
S2			125 (6)*	7 (9)	132 (9)
S3	118 (20)	114 (4)	121 (5)	8 (5)	129 (6)

Values are means (SD) in mmHg. MAP, mean arterial pressure. *Significant difference between S1 and S2 ($P < 0.05$, ANOVA for repeated measures and Tukey post hoc analysis).

Table 4. *Parameter estimates of leg VC during three moderate-intensity knee-extension exercise transitions*

Protocol	Rest, ml·min^{-1}·mmHg^{-1}	Passive, ml·min^{-1}·mmHg^{-1}	BL, ml·min^{-1}·mmHg^{-1}	Amp, ml·min^{-1}·mmHg^{-1}	TD, s	τ, s	EE VC, ml·min^{-1}·mmHg^{-1}
S1	2.4 (0.4)	3.6 (0.8)	8.7 (0.7)*	4.3 (0.3)†	5 (3)	16 (3)*	13.1 (0.7)*†
S2			13.1 (0.7)*‡	4.1 (1.3)‡	1 (8)	34 (15)*‡	17.2 (1.3)*
S3	2.2 (0.4)	3.4 (1.0)	8.8 (1.3)‡	7.6 (1.3)†‡	3 (3)	17 (4)‡	16.5 (0.6)†

Values are means (SD). VC, vascular conductance. Significant difference between *S1 and S2, †S1 and S3, and ‡S2 and S3 ($P < 0.05$ ANOVA for repeated measures and Tukey post hoc analysis).

~1.1 and ~2.2 l/min for $\dot{V}O_2$ and LBF, respectively. These findings are somewhat higher than values during two-legged KE exercise at ~40 W, reported previously by MacDonald et al. (26) ($\dot{V}O_2$, 0.9 l/min; LBF, 2.0 l/min) and Shoemaker et al. (36) ($\dot{V}O_2$, 1.0 l/min; LBF, ~0.7 l/min, calculated from MBV and an assumed arterial diameter = 10 mm). Differences between studies might be explained by slight differences in the KE ergometer and the KE protocol. The mean femoral arterial diameter reported in this study (~10 mm) and the observation that arterial diameter does not change significantly during the rest-exercise transition agrees with previously published reports (26, 28, 29).

In the present study, the steady-state functional G ($\Delta\dot{V}O_2/\Delta WR$) of the $\dot{V}O_2$ response was greater in S2 compared with S1, consistent with our laboratory's previous study performed by using leg cycle ergometry (8). The functional G in each of the regions during KE exercise (S1, ~13.5 ml·min^{-1}·W^{-1}; S2, ~18.1 ml·min^{-1}·W^{-1}) appeared greater than values normally reported for leg cycling exercise [e.g., S1, ~10.6 ml·min^{-1}·W^{-1}; S2, ~11.9 ml·min^{-1}·W^{-1} (8)], but is consistent with previous reports of a greater O_2 cost per WR for KE exercise (1, 2, 15, 25, 31) compared with leg cycling exercise (25, 40, 41). For example, Koga et al. (25) directly compared KE and leg cycling exercise and reported a higher $\dot{V}O_2$ G during KE (~12 ml·min^{-1}·W^{-1}) compared with leg cycling exercise (~9 ml·min^{-1}·W^{-1}), regardless of whether the exercise was performed at the same absolute (i.e., 66 W) or relative intensity (KE, 38 W; leg cycling, 66 W). It is not clear why the $\dot{V}O_2$ G is greater in KE than leg cycling exercise; however, muscle work during KE exercise is restricted mainly to the quadriceps muscle group, whereas a number of muscles groups, including muscles of the upper and lower leg, are recruited during leg cycling exercise (1, 21, 30), and thus differences may relate to the combined metabolic and/or mechanical efficiencies of the muscles used during the different exercise modes.

In the present study, the finding that $\dot{V}O_2$ kinetics were slower in S2 compared with S1 is in agreement with previous reports (8, 13, 22), but is not consistent with the findings showing either a faster adaptation (12) or no difference in the $\dot{V}O_2$ kinetic response (10) when exercise was initiated from prior exercise compared with rest.

The factors responsible for limiting the rate of $\dot{V}O_2$ adaptation during the transition toward a new exercise steady-state broadly are categorized as being related to limitations imposed by *1*) the adaptation of muscle blood flow and muscle O_2 delivery, and *2*) the activation of muscle enzymes and provision of substrates (other than O_2) to the mitochondrial TCA cycle and electron transport chain (16, 24, 37). Hughson and Morrissey (22, 23) suggested that the slower adaptation of $\dot{V}O_2$ in the S2 compared with S1 could be a consequence of an O_2 transport limitation, as suggested by slower HR kinetics (i.e., greater HR MRT) (23). In agreement, in the present study, the HR kinetics were slower in the S2 (τHR ~42 s) compared with the S1 (τHR ~21 s) transition to exercise (Table 2). In the present study, we extended these observations to show that the adaptation of femoral artery blood flow and VC also were slower when exercise was initiated in the upper (τLBF ~39 s; τVC, 34 s) compared with the lower region (τLBF ~21 s; τVC, 16 s) of the moderate-intensity domain (Tables 2 and 4), and that the increase in LBF for a given increase in $\dot{V}O_2$ (and WR) was less in S2 ($\Delta LBF \cdot 2/\Delta\dot{V}O_2$, 4.6 l·min·l^{-1}·min^{-1}) compared with S1 (5.7 l·min·l^{-1}·min^{-1}) (Table 2). Also, a higher NIRS-derived HHb signal before the onset of the S2 transition and greater HHb Amp likely reflect a lower microvascular P_{O_2}, which would lower the O_2 driving pressure from the microvasculature to the muscle mitochondria and possibly provide an additional "diffusive" limitation to $\dot{V}O_2$ kinetics (27), thereby possibly requiring a greater O_2 extraction (seen here as a greater HHb Amp and $\Delta HHb/\Delta\dot{V}O_2$ ratio in S2), a greater blood-tissue O_2 conductivity, and/or greater substrate level phosphorylation. Thus the slower adaptation of HR and LBF (and VC) in S2 (and lower microvascular P_{O_2}), along with a slower adaptation of $\dot{V}O_2$ in this region, is consistent with $\dot{V}O_2$ kinetics being limited by muscle blood flow and/or convective (and possibly diffusive) O_2 transport in this region.

The higher BL HR and slower HR kinetics during the exercise transition in the upper region of the moderate domain are consistent with reduced parasympathetic control of HR in this region (32). To our knowledge, this is the first study to show that LBF adapts more slowly and with an attenuated steady-state rise (relative to $\dot{V}O_2$) when the exercise transition is initiated from a BL of prior moderate-intensity exercise. The time course of adaptation of LBF and HR (i.e., τLBF and τHR, respectively) were similar during each of the exercise transitions (Fig. 6), suggesting the adaptation of LBF, in part, was related to adaptations in HR (and presumably cardiac output). Also, while leg VC increased during each of the exercise transitions, the kinetics of leg VC (and thus leg vasodilation) was slower in S2. In contrast, Saunders et al. (33) observed an immediate, "fast" (phase I) increase in forearm VC, which was delayed and slower during a transition from rest to a WR exhibiting 40% peak VC (rest to 40%) compared with a transition from 40-to-80% peak VC. Also, in that study, a second, "slower" (phase II) increase in forearm VC was delayed in onset during the 40-to-80% peak VC transition compared with the rest-to-40% transition, but the Amp and the kinetics of the increase in VC were not different between transitions (33). However, in that study, $\dot{V}O_2$ or forearm blood flow data were not presented to determine whether the adaptation of these variables differed between the two exercise transitions. Methodological differences that might account for

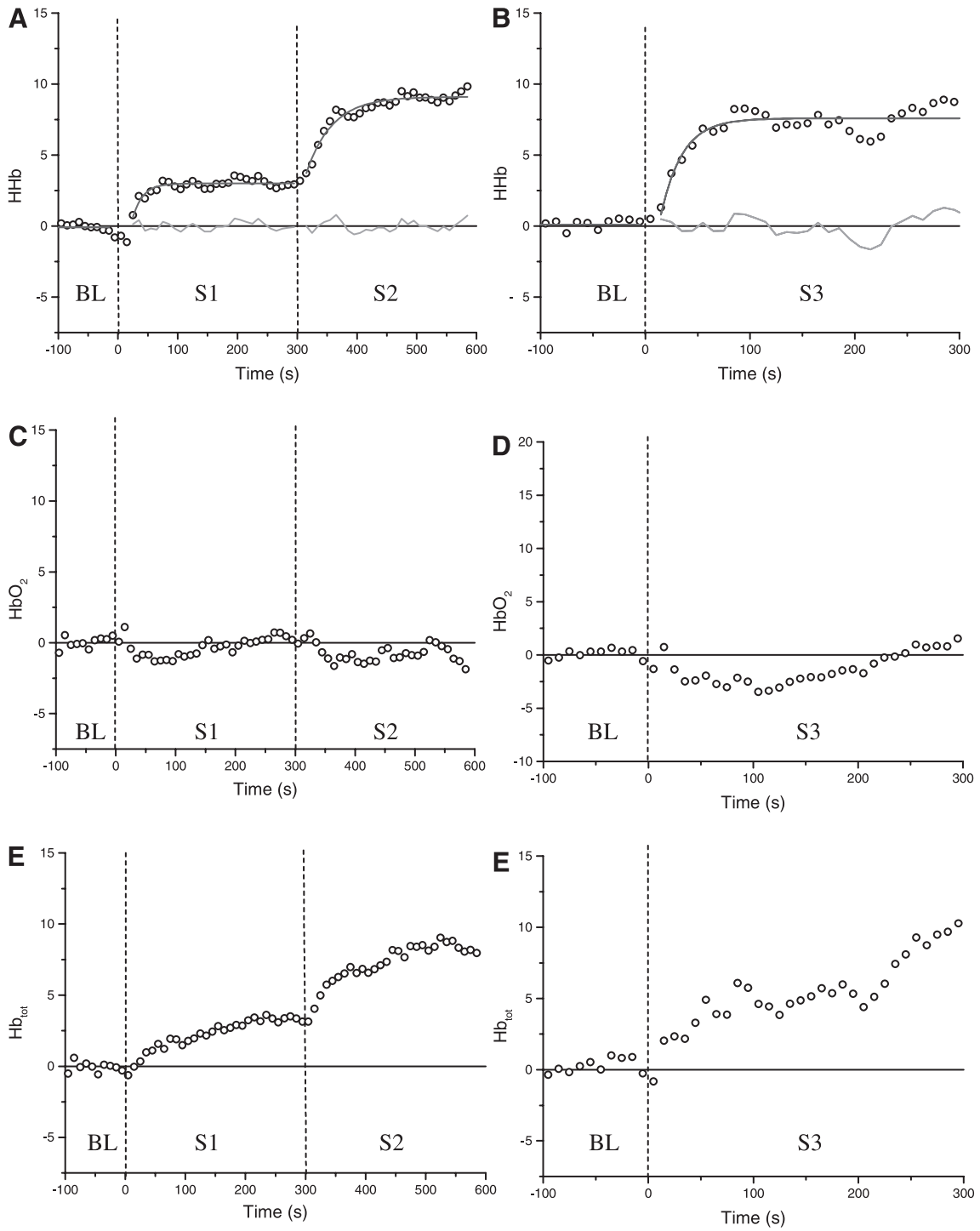

Fig. 5. Adaptation of the normalized concentration changes of HHb (*A* and *B*), oxyhemoglobin (HbO_2; *C* and *D*), and total hemoglobin (Hb_{tot}; *E* and *F*) to a double- (S1, S2) and single-step (S3) protocols. Also shown is the line of best fit and residuals of the monoexponential fit for the HHb response. The response profile represents an average of 6 trials, with each datum presented as a 10-s average of 1-s interpolated data. Dashed lines indicate a transition in exercise intensity.

the different findings between the present study and that of Saunders et al. (33) include *1*) the use of a different muscle group and exercise modality (i.e., intermittent forearm handgrip exercise vs. KE exercise); *2*) the lower transition was initiated from a BL of rest rather than light-intensity exercise, and thus the initial changes in VC (and presumably blood flow) would be greater and perhaps reflect slight differences in response to those factors (i.e., mechanical, chemical), contributing to the initial vascular smooth muscle relaxation; and *3*) the intensity used in the upper transition (i.e., 80% VC peak) appeared to be in the heavy-intensity domain, rather than moderate-intensity used in this study, as a steady-state was not

Table 5. *Parameter estimates of normalized muscle HHb during three moderate-intensity knee-extension exercise transitions*

Protocol	BL, OD units	Amp, ΔOD units	TD, s	τ, s	C_{95}, s	MRT, s	EE HHb, ΔOD units	ΔHHb/Δ$\dot{V}O_2$, OD units·l^{-1}·min^{-1}
S1	0.01 (0.06)*	2.70 (1.03)*†	20 (4)*	16 (6)*	5 (2)	36 (7)*	2.71 (1.05)*†	13.2 (5.6)*
S2	2.71 (1.05)*‡	5.22 (1.53)*	14 (7)*	33 (11)*‡	4 (2)	47 (10)*‡	7.92 (2.27)*	18.8 (5.5)*‡
S3	0.04 (0.04)‡	6.63 (1.92)†	17 (3)	14 (5)‡	5 (2)	31 (4)‡	6.67 (1.92)†	14.6 (4.8)‡

Values are means (SD). OD, optical density; MRT, mean response time (TD + τ); HHb, deoxyhemoglobin. Significant difference between *S1 and S2, †S1 and S3, and ‡S2 and S3 ($P < 0.05$ ANOVA for repeated measures and Tukey post hoc analysis).

reached or was delayed because of an additional delayed increase in VC.

Increases in muscle blood flow at exercise onset are related to the mechanical effect of muscle contraction and activation of muscle pump activity and vasodilation and increases in VC (39). Tschakovsky and colleagues observed a rapid vasodilation within the first relaxation cycle after a single forearm contraction (34, 38, 39), and while this immediate increase in VC was identical in rest-to-mild and mild-to-moderate intensity forearm exercise transitions, a blunted response was seen with the forearm below compared with above heart level (34). Also, while VC increased further with continued contractions in both arm positions, the VC response with the forearm below heart level was attenuated in the mild-to-moderate compared with the rest-to-mild intensity condition, but was similar in both transitions with the forearm above heart level (34). In the present study, although the kinetics of the increase in VC were slower in the S2 transition, the VC Amp was not different between the two transitions, despite the exercise being performed below heart level.

Increases in VC reflect the balance between vasoconstrictor and vasodilatory influences on the vascular smooth muscle. Matching of blood flow to metabolic demand likely involves release of vasodilator substances from active fibers (e.g., acetylcholine, adenosine, nitric oxide, K^+, prostagladins, CO_2, hydrogen ions, endothelial-derived hyperpolarizing factor) and transmission of the dilatory signal to upstream resistance vessels (by direct coupling between endothelial cells and/or smooth muscle). Whether differences in the time course of appearance and accumulation in the concentration of vasodilator substances, or their efficacy on the activation of signaling pathways leading to vascular smooth muscle relaxation, can account for the slowed LBF and VC response seen in S2 compared with S1 in the present study is unknown, as no studies have yet examined the release of these substances in different regions of the moderate-intensity domain. However,

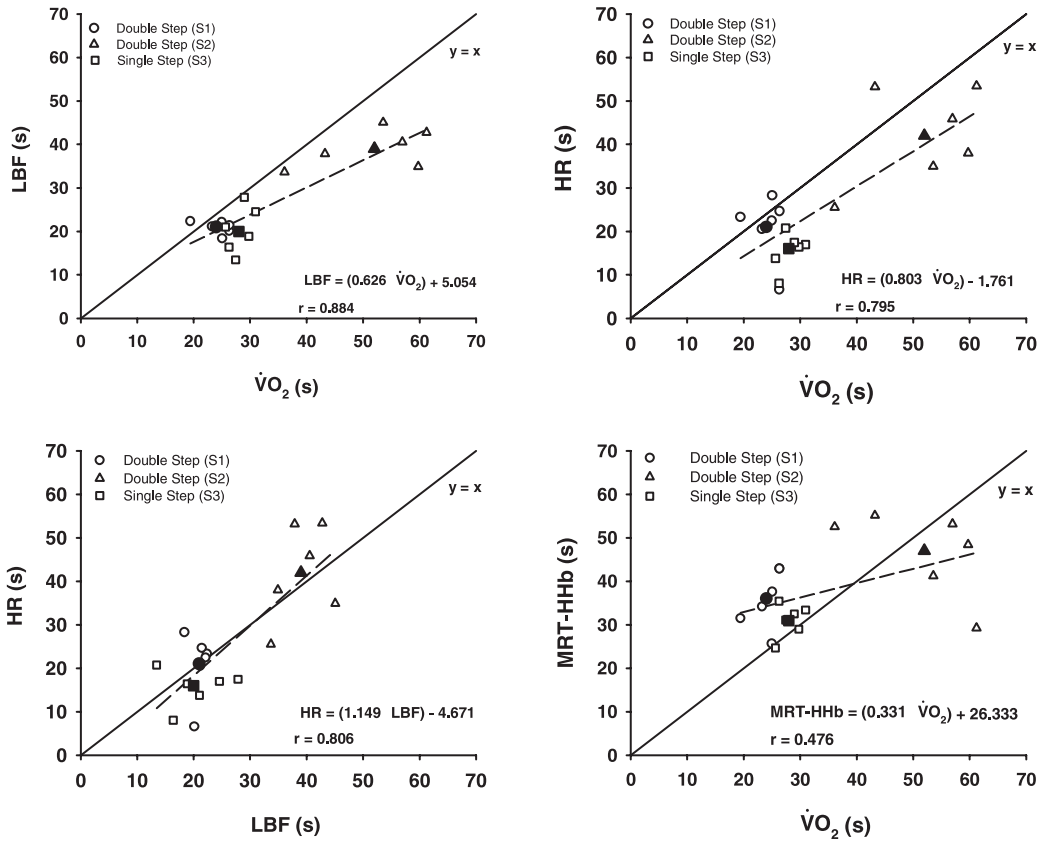

Fig. 6. Relationship between the adaptations of pulmonary $\dot{V}O_2$ ($\tau\dot{V}O_2$), femoral arterial blood flow (τLBF), HR (τHR), and HHb [mean response time (MRT)-Hb] during double-step (S1, circles; S2, triangles) and single-step (S3, squares) transitions within the moderate-intensity exercise domain. Individual (open symbols) and group mean (solid symbols) responses are presented.

the similarity between τLBF and τHR (and its effect on cardiac output) seen between each of the exercise transitions suggests some correspondence between the two variables, either directly through bulk flow delivery, or indirectly through effects on shear stress. It is unlikely that a single factor contributes to the increase in VC and its time course during the exercise transition, and it is possible that the relative roles and contributions of the various factors may change with exercise intensity and duration [as suggested by Tschakovsky and Sheriff (39)].

The slower $\dot{V}O_2$ response coincident with a slower LBF and HR response is consistent with an O_2 transport limitation to $\dot{V}O_2$ in S2. However, Grassi and coworkers (17, 18) argued against an O_2 delivery limitation to $\dot{V}O_2$ kinetics during moderate-intensity exercise in an isolated canine gastrocnemius muscle preparation. In those studies, convective O_2 delivery (via pump perfusion and adenosine-induced vasodilation) (17) or combined convective and diffusive O_2 delivery [increased HbO_2 half-saturation pressure (by RSR-13 infusion) and hyperoxia] (18) were elevated before the onset of electrically stimulated muscle contractions and were found not to speed $\dot{V}O_2$ kinetics during the subsequent exercise transient. Direct comparisons regarding limiting factors at exercise onset between those studies and the present one, however, should be made with caution, as the electrically stimulated canine hindlimb model used by Grassi and coworkers (17, 18) offers differences in muscle morphology (greater fiber type I, IIa homogeneity; greater oxidative capacity), muscle fiber recruitment (because of electrical stimulation), and microvascular supply (greater muscle capillarization) and recruitment (because of maximal adenosine-induced vasodilation) compared with the adaptations expected at the start of exercise in humans.

Doppler ultrasonography measures blood flow of the conduit artery supplying the exercising muscle; however, the NIRS-derived HHb signal represents a balance between local muscle blood flow (and O_2 delivery) and muscle utilization within a specific region of the active muscle. In the present study, despite a slower LBF response in S2 (and similar Amp of LBF increase), the TD before an increase in muscle deoxygenation (HHb) was reduced in S2 (~14 s) compared with S1 (~20 s), and the HHb-Amp was greater (S2, 5.2 ΔOD units; S1, 2.7 ΔOD units), suggesting a greater mismatch between local blood flow distribution and O_2 utilization earlier in the S2 transition, with muscle O_2 utilization increasing by means of a greater O_2 extraction, as local blood flow was slowed. The TD of the NIRS-derived muscle HHb during the initial phase of the exercise transition reported in the present investigation is consistent with the findings from previous studies (9, 19). The higher steady-state G ($\Delta\dot{V}O_2/\Delta WR$) in S2 (18.1 $ml \cdot min^{-1} \cdot W^{-1}$) than S1 (13.5 $ml \cdot min^{-1} \cdot W^{-1}$) and lower steady-state LBF-to-$\dot{V}O_2$ increase in S2 supports the contention that the activation of muscle O_2 consumption in the upper region of the moderate-intensity domain was greater than that of blood flow, requiring increased O_2 extraction to meet the O_2 demands of the exercising muscle.

Recent studies by Poole and colleagues show that there is a transient undershoot in microvascular P_{O_2} at the onset of electrically stimulated muscle contractions (reflecting a greater muscle O_2 utilization relative to muscle microvascular blood flow) in exposed muscle from animals with disease (6, 11), muscle from old vs. young animals (5), and in muscles having a higher fast- vs. slow-twitch fiber composition (27). In accordance with the data on microvascular P_{O_2} profiles, a transient overshoot in the HHb response might be expected whenever the adaptation of muscle O_2 consumption exceeds that of microvascular blood flow. In examining our data (both on individual and ensemble-averaged responses across a number of studies), an overshoot in HHb response reflecting the rather dramatic undershoot that is seen in the microvascular P_{O_2} profiles reported by Behnke et al. (see Fig. 3 in Ref. 6 and Fig. 2 in Ref. 5) and McDonough et al. (see Fig. 1 in Ref. 27) is seldom seen. However, in our analysis, we average data into 5- or 10-s time bins to reduce variability in the profiles that may obscure any overshoot that might exist during the exercise transient. Also, Poole and colleagues (5, 6, 11, 27) use an exposed, in situ animal muscle preparation to study microvascular P_{O_2}, whereas we study NIRS-derived HHb changes measured on the skin surface above the quadriceps muscle during human exercise, where the fidelity of the response may not be as great. In general the NIRS-derived HHb signal adapts with an "exponential-like" profile that we find can be fit adequately using a monoexponential model (see Fig. 5).

A slowing of $\dot{V}O_2$ kinetics in the upper compared with lower regions of the moderate-intensity domain also may be attributed to an intrinsic slowness in activating intracellular oxidative metabolism in response to the new metabolic requirement in S2 and may involve a slowed activation of muscle enzymes and/or slowed or inadequate provision of substrates for mitochondrial respiration; e.g., delayed activation of the pyruvate dehydrogenase complex resulting in inadequate provision of acetyl-CoA to the TCA cycle and thus reducing equivalents (i.e., NADH) and electrons to the electron transport chain. The authors are not aware of any studies that have examined the time course of oxidative enzyme activation and substrate provision in different regions of the moderate-intensity domain. Alternatively, the slowed $\dot{V}O_2$ response may be related to the inherent O_2 use and efficiency characteristics of the muscle fibers recruited in the different regions of the moderate-intensity domain, with high efficient fibers (with fast O_2 utilization profiles) being recruited initially (i.e., in the lower region of the moderate-intensity domain), and less efficient fibers (with slower O_2 utilization profiles) recruited with transitions to higher WRs (i.e., in the upper region of the moderate-intensity domain) (as suggested in Ref. 8).

Methodological Considerations

The kinetics of measured pulmonary $\dot{V}O_2$ is used to reflect muscle O_2 consumption. The close approximation between phase II pulmonary $\dot{V}O_2$ and muscle O_2 consumption has been confirmed by using computer modeling simulations (3) and in direct comparisons of pulmonary $\dot{V}O_2$ and leg muscle O_2 consumption (using LBF measured by thermodilution and measured arteriovenous O_2 content differences) during leg cycling exercise in humans (20).

NIRS is used to study local HbO_2 and HHb changes within small regions of active muscle. Specifically, it is assumed that changes in the NIRS-HHb signal reflect the balance between local muscle O_2 utilization and local microvascular perfusion within the NIRS field of interrogation. Also, the NIRS signals, while measuring changes only within a small region of muscle, are assumed to reflect changes occurring within the whole

muscle group. Finally, the relative contribution of arterioles, capillaries, and venules to the NIRS HHb signal is assumed to remain constant during the exercise transitions and to reflect changes in O_2 extraction by the active tissue. These limitations cannot presently be resolved; however, the temporal profiles of NIRS HHb (this study) and measures of microvascular P_{O_2} (e.g., Refs. 5, 6, 27) and arteriovenous O_2 content differences (e.g., Ref. 20) suggest that the NIRS HHb signal provides a good approximation of muscle O_2 extraction and utilization profiles.

In summary, this study has confirmed the slower $\dot{V}O_2$ response in the upper compared with the lower region of the moderate-intensity exercise domain in young, healthy adults. The slowed $\dot{V}O_2$ kinetics were accompanied by slower HR, leg muscle conduit artery blood flow, and VC kinetics, lower $\Delta(LBF \cdot 2)/\Delta\dot{V}O_2$ and greater HHb Amp response in the upper region, consistent with a mechanism whereby $\dot{V}O_2$ kinetics in this upper region are limited, at least in part, by blood flow and/or O_2 transport. The NIRS-derived HHb data suggest that O_2 extraction was increased in S2, thereby compensating for the slower and/or lower LBF response and, consequently, preventing a further slowing of the $\dot{V}O_2$ time course. However, because information on enzyme activation and substrate provision is limited for exercise performed in different regions of the moderate-intensity domain, a role for metabolic inertia cannot be ruled out.

ACKNOWLEDGMENTS

Technical support of Brad Hansen was greatly appreciated.

GRANTS

This study was supported by Natural Sciences and Engineering Research Council of Canada research and equipment grants. Additional support was provided by The University of Western Ontario Academic Development Fund and infrastructure support from the Canadian Foundation for Innovation and Ontario Innovation Trust.

REFERENCES

1. **Andersen P, Adams RP, Sjögaard G, Thorboe A, and Saltin B.** Dynamic knee extension as model for study of isolated exercising muscle in humans. *J Appl Physiol* 59: 1647–1653, 1985.
2. **Andersen P and Saltin B.** Maximal perfusion of skeletal muscle in man. *J Physiol* 366: 233–249, 1985.
3. **Barstow TJ, Lamarra N, and Whipp BJ.** Modulation of muscle and pulmonary O_2 uptakes by circulatory dynamics during exercise. *J Appl Physiol* 68: 979–989, 1990.
4. **Beaver WL, Lamarra N, and Wasserman K.** Breath-by-breath measurement of true alveolar gas exchange. *J Appl Physiol* 51: 1662–1675, 1981.
5. **Behnke BJ, Delp MD, Dougherty PJ, Musch TI, and Poole DC.** Effects of aging on microvascular oxygen pressures in rat skeletal muscle. *Respir Physiol Neurobiol* 146: 259–268, 2005.
6. **Behnke BJ, Kindig CA, McDonough P, Poole DC, and Sexton WL.** Dynamics of microvascular oxygen pressure during rest-contraction transition in skeletal muscle of diabetic rats. *Am J Physiol Heart Circ Physiol* 283: H926–H932, 2002.
7. **Bell C, Paterson DH, Kowalchuk JM, Moy AP, Thorp DB, Noble EG, Taylor AW, and Cunningham DA.** Determinants of oxygen uptake kinetics in older humans following single-limb endurance exercise training. *Exp Physiol* 86: 659–665, 2001.
8. **Brittain CJ, Rossiter HB, Kowalchuk JM, and Whipp BJ.** Effect of prior metabolic rate on the kinetics of oxygen uptake during moderate-intensity exercise. *Eur J Appl Physiol* 86: 125–134, 2001.
9. **DeLorey DS, Kowalchuk JM, and Paterson DH.** Relationship between pulmonary O_2 uptake kinetics and muscle deoxygenation during moderate-intensity exercise. *J Appl Physiol* 95: 113–120, 2003.
10. **Diamond LB, Casaburi R, Wasserman K, and Whipp BJ.** Kinetics of gas exchange and ventilation in transitions from rest or prior exercise. *J Appl Physiol* 43: 704–708, 1977.
11. **Diederich ER, Behnke BJ, McDonough P, Kindig CA, Barstow TJ, Poole DC, and Musch TI.** Dynamics of microvascular oxygen partial pressure in contracting skeletal muscle of rats with chronic heart failure. *Cardiovasc Res* 56: 479–486, 2002.
12. **DiPrampero PE, Davies CTM, Cerretelli P, and Margaria R.** An analysis of O_2 debt contracted in submaximal exercise. *J Appl Physiol* 29: 547–551, 1970.
13. **DiPrampero PE, Mahler PB, Giezendanner D, and Cerretelli P.** Effects of priming exercise on $\dot{V}O_2$ kinetics and O_2 deficit at the onset of stepping and cycling. *J Appl Physiol* 66: 2023–2031, 1989.
14. **Elwell CE.** *A Practical Users Guide to Near Infrared Spectroscopy*. London: Hamamatsu Photonics KK, 1995, p. 1–155.
15. **Ferguson RA, Aagaard P, Ball D, Sargeant AJ, and Bangsbo J.** Total power output generated during dynamic knee extensor exercise at different contraction frequencies. *J Appl Physiol* 89: 1912–1918, 2000.
16. **Grassi B.** Regulation of oxygen consumption at exercise onset: is it really controversial? *Exerc Sport Sci Rev* 29: 134–138, 2001.
17. **Grassi B, Gladden LB, Samaja M, Stary CM, and Hogan MC.** Faster adjustments of O_2 delivery does not affect $\dot{V}O_2$ on-kinetics in isolated in situ canine muscle. *J Appl Physiol* 85: 1394–1403, 1998.
18. **Grassi B, Gladden LB, Stary CM, Wagner PD, and Hogan MC.** Peripheral O_2 diffusion does not affect $\dot{V}O_2$ on-kinetics in isolated in situ canine muscle. *J Appl Physiol* 85: 1404–1412, 1998.
19. **Grassi B, Pogliaghi S, Rampichini S, Quaresima V, Ferrari M, Marconi C, and Cerretelli P.** Muscle oxygenation and pulmonary gas exchange kinetics during cycling exercise on-transitions in humans. *J Appl Physiol* 95: 149–158, 2003.
20. **Grassi B, Poole DC, Richardson RS, Knight DR, Erickson BK, and Wagner PD.** Muscle O_2 uptake kinetics in humans: implications for metabolic control. *J Appl Physiol* 80: 988–998, 1996.
21. **Green HJ and Patla AE.** Maximal aerobic power: neuromuscular and metabolic considerations. *Med Sci Sports Exerc* 24: 38–46, 1992.
22. **Hughson RL and Morrissey M.** Delayed kinetics of respiratory gas exchange in the transition from prior exercise. *J Appl Physiol* 52: 921–929, 1982.
23. **Hughson RL and Morrissey M.** Delayed kinetics of $\dot{V}O_2$ in the transition from prior exercise. Evidence for O_2 transport limitation of $\dot{V}O_2$ kinetics: a review. *Int J Sports Med* 4: 31–39, 1983.
24. **Hughson RL, Tschakovsky ME, and Houston ME.** Regulation of oxygen consumption at the onset of exercise. *Exerc Sport Sci Rev* 29: 129–133, 2001.
25. **Koga S, Poole DC, Shiojiri T, Kondo N, Fukuba Y, Miura A, and Barstow TJ.** Comparison of oxygen uptake kinetics during knee extension and cycle exercise. *Am J Physiol Regul Integr Comp Physiol* 288: R212–R220, 2005.
26. **MacDonald MJ, Shoemaker JK, Tschakovsky ME, and Hughson RL.** Alveolar oxygen uptake and femoral artery blood flow dynamics in upright and supine leg exercise in humans. *J Appl Physiol* 85: 1622–1628, 1998.
27. **McDonough P, Behnke BJ, Padilla DJ, Musch TI, and Poole DC.** Control of microvascular oxygen pressures in rat muscles comprised of different fibre types. *J Physiol* 563: 903–913, 2005.
28. **Rådegran G.** Ultrasound Doppler estimates of femoral artery blood flow during dynamic knee extensor exercise in humans. *J Appl Physiol* 83: 1383–1388, 1997.
29. **Rådegran G and Saltin B.** Muscle blood flow at onset of dynamic exercise in man. *Am J Physiol Heart Circ Physiol* 274: H314–H322, 1998.
30. **Richardson RS, Frank LR, and Haseler LJ.** Dynamic knee-extensor and cycle exercise: functional MRI of muscular activity. *Int J Sports Med* 19: 182–187, 1998.
31. **Richardson RS, Poole DC, Knight DR, Kurdak SS, Hogan MC, Grassi B, Johnson EC, Kendrick KF, Erickson BK, and Wagner PD.** High muscle blood flow in man: is maximal O_2 extraction compromised? *J Appl Physiol* 75: 1911–1916, 1993.
32. **Rowell LB.** *Human Cardiovascular Control*. New York: Oxford University Press, 1993, p. 1–500.
33. **Saunders NR, Pyke KE, and Tschakovsky ME.** Dynamic response characteristics of local muscle blood flow regulatory mechanisms in human forearm exercise. *J Appl Physiol* 98: 1286–1296, 2005.
34. **Saunders NR and Tschakovsky ME.** Evidence for a rapid vasodilatory contribution to immediate hyperemia in rest-to-mild and mild-to-moderate forearm exercise transitions in humans. *J Appl Physiol* 97: 1143–1151, 2004.

35. **Scheuermann BW, Bell C, Paterson DH, Barstow TJ, and Kowalchuk JM.** Oxygen uptake kinetics for moderate exercise are speeded in older humans by prior heavy exercise. *J Appl Physiol* 92: 609–616, 2002.
36. **Shoemaker JK, Hodge L, and Hughson RL.** Cardiorespiratory kinetics and femoral artery blood velocity during dynamic knee extension exercise. *J Appl Physiol* 77: 2625–2632, 1994.
37. **Tschakovsky ME and Hughson RL.** Interaction of factors determining oxygen uptake at the onset of exercise. *J Appl Physiol* 86: 1101–1113, 1999.
38. **Tschakovsky ME, Rogers AM, Pyke KE, Saunders NR, Glenn N, Lee SJ, Weissgerber T, and Dwyer EM.** Immediate exercise hyperemia in humans is contraction intensity dependent: evidence for rapid vasodilation. *J Appl Physiol* 96: 639–644, 2004.
39. **Tschakovsky ME and Sheriff DD.** Immediate exercise hyperemia: contributions of the muscle pump vs. rapid vasodilation. *J Appl Physiol* 97: 739–747, 2004.
40. **Wasserman K, Hansen JE, Sue DY, Casaburi R, and Whipp BJ.** *Principles of Exercise Testing and Interpretation Including Pathophysiology and Clinical Applications*. Philadelphia, PA: Lippincott Williams and Wilkins, 2005, p. 1–585.
41. **Wells R, Morrissey M, and Hughson R.** Internal work and physiological responses during concentric and eccentric cycle ergometry. *Eur J Appl Physiol* 55: 295–301, 1986.
42. **Wesche J.** The time course and magnitude of blood flow changes in the human quadriceps muscles following isometric contraction. *J Physiol* 377: 445–462, 1986.